Determining soil erosion by water using high resolution remotely-sensed data

MAGDALENA FITRZYK

Institute of Geodesy and Geoinformatics, Wroclaw University of Environmental and Life Sciences, Grunwaldzka 53, 50-357 Wroclaw, Poland
magdalena.fitrzyk@igig.up.wroc.pl

Abstract The Trzebnickie Hills located to the north of Wroclaw, Poland, are dominated by fertile loess soil formations which are highly susceptible to water erosion. Against this context, the aim of this study was to investigate the advantages and limitations of using satellite imagery in the assessment of water erosion of loess soils. More specifically, the work focused on the interferometric analysis of high resolution SAR images from the TerraSAR-X satellite using coherence imagery. The results of this analysis were superimposed on a digital elevation model and slopes map to assess the relationship with coherence loss. Both visual interpretation and statistical analysis demonstrated that there may be correlation between local terrain slope angles and decreased correlation in coherence maps. Since slope is a major trigger of soil denudation, it was concluded that coherence maps can serve as a useful tool for extracting and delineating eroded areas. However, certain conditions must be met before the assessment of erosion from coherence maps can be considered credible and these are briefly discussed.

Key words loess soils erosion; TerraSAR-X; interferometry

INTRODUCTION

The Trzebnickie Hills in the northern part of Lower Silesia province, to the north of the city of Wroclaw, Poland, are dominated by fertile loess formations. Extensive soil erosion results from a combination of the high susceptibility of the local loess soils to water erosion and the agricultural land use. Extensive cultivation and widespread down slope tillage facilitate the transport of mobilized soil particles during heavy rains and snowmelts. The soil water erosion leads to soil depletion, reduced crop yields, degraded water quality, changes in drainage patterns and generates serious local economic problems. Previous work has reported the magnitude and extent of soil erosion by water in the study area, including the study by Szewrański & Żmuda (2008) which proposed and assessed erosion mitigation scenarios using a modelling approach.

Collecting reliable data on soil erosion by water using conventional approaches is costly and time-consuming. According to Vierling (2006) there are three basic approaches to soil erosion spatial assessment:

(a) field measurements at different locations;
(b) direct surveys of erosion features such as rills and gullies;
(c) modelling based on the integration of spatial data.

Limited empirical data and the costs of direct surveys can hamper the reliable spatial assessment of soil erosion by water, especially at larger spatial scales. In such cases, existing assessment methods and techniques can be supported by satellite data. Satellite imagery is increasingly being used to detect eroded areas or to assess the key factors that influence erosion, including slope, vegetation cover and soil characteristics. The most often used type of satellite data are images from optical sensors such as Landsat, SPOT, ASTER, or the higher resolution QuickBird and IKONOS. These are passive sensors that do not transmit their own signal, but instead measure the reflection of sunlight in the visible and infrared parts of the electromagnetic spectrum and thermal infrared radiance, thereby being day/night and weather dependent. In contrast, active sensors (i.e. radars) transmit microwaves and record the received signal and can operate regardless of weather conditions and sunlight. In this context, the potential of employing radar satellite data to detect soil erosion was studied using interferometric processing of complex SAR (Synthetic Aperture Radar) images obtained with the high resolution TerraSAR-X satellite in April 2011. The results of this research represent part of a larger study integrating remotely sensed data and soil erosion assessment.

Copyright © 2012 IAHS Press

MATERIALS AND METHODS

Synthetic aperture radar (SAR) complex images are commonly used in studies of the surface of the Earth. There are various methods and algorithms for processing the data acquired by SAR sensors which yield information useful in the detection of features, properties and changes in the Earth's surface. In terms of the research presented in this paper, SAR can provide the vital data used in the detection of soil erosion by water. Terrain slopes, traditionally obtained from topographic maps or aerial photogrammetry, can be easily determined from accurate Digital Elevation Models (DEM) developed from SAR images (e.g. Rabus *et al*., 2003). Other spatial data frequently used as input in erosion models can be derived from SAR, including land use and vegetation, soil properties, cropping and tillage methods. Depending on the purpose of the work and spatial extent of the phenomenon analysed, different resolutions of SAR images may be used, from lower resolution ERS or ENVISAT (~30 m) to high resolution TerraSAR-X images obtained in Spotlight mode (1 m).

A widely-used technique for detecting change in terrain is Interferometric Synthetic Aperture Radar (abbreviated as InSAR). In this method, two complex images acquired by a spaceborne synthetic aperture radar at two distinct times from a similar viewing geometry are used to compute the interference pattern caused by the difference in the phase of the reflected radar waves. The resulting interferogram is a contour map of changes in distance between the ground and the radar instrument (Massonnet & Feigl, 1998). SAR interferometry is being successfully applied to detect small changes in topography caused, for example, by earthquakes and land subsidence. The basic principles of InSAR and its use are reported by Massonnet & Feigl (1998) and Perski (2003) and demonstrated in Fig. 1. Despite its substantial potential for detecting small topographical changes, SAR interferometry has limitations because to obtain good quality interferometric patterns (fringes) high level coherence of the radar images is required. Coherence is basically the correlation coefficient between radar images and will be discussed in subsequent sections. When the scattering mechanism in the resolution cell between two images is disturbed – which means that the coherence is lost – the phase difference between two complex images cannot be determined and the interferometric patterns become very noisy or cannot be resolved at all.

Coherence loss can be attributed to a range of factors such as the topography of the area, terrain slope, imaging geometry and receiver noise. However, precipitation and more specifically soil humidity are major reasons for the decorrelation between SAR images. As a result, the inteferometric method is limited to areas where the eroded top soil layer is homogenous and arid (Wegmuller *et al*., 2000) and cannot be effectively applied in areas where erosion is induced by water.

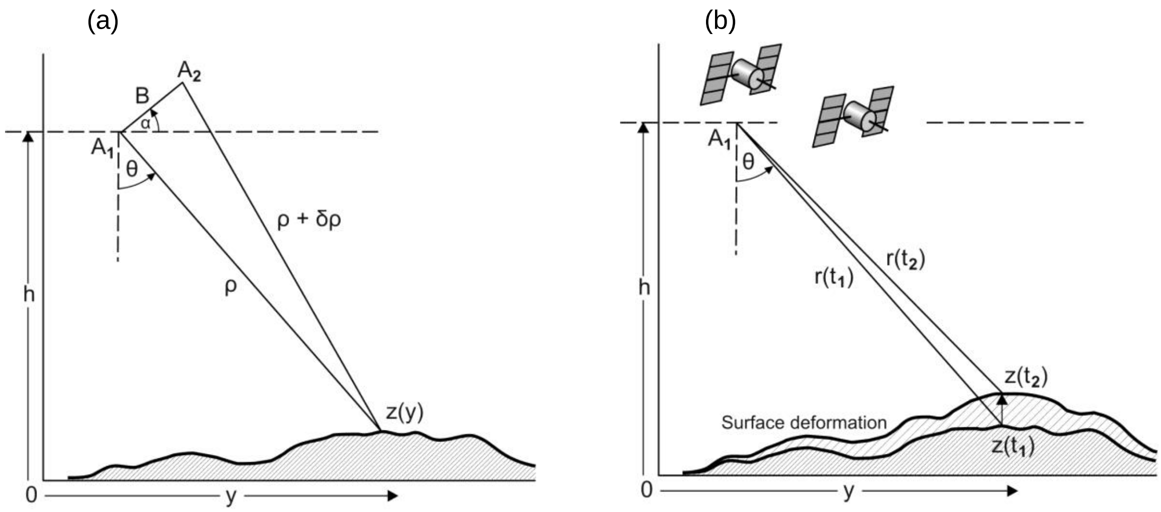

Fig. 1 (a) The principle of InSAR. Single pass: two antenna at different locations A_1 and A_2 are used to determine the topography z(y). Source: ESA. (b) The principle of repeat pass InSAR. Repeat pass: repeat passes of a radar instrument in A1 are used to determine the deformation between t_1 and t_2. Adapted from ESA.

Against the above background, this study aimed to explore the possibility of applying the analysis of coherence itself to the spatial assessment of soil erosion intensity and to the identification of erosion features such as rills and gullies. More specifically, the work investigated whether the visual and statistical interpretation of highly decorrelated images can reveal the occurrence of soil erosion by water. The assessment used high resolution satellite radar data from the TerraSAR-X satellite. TerraSAR-X is an active radar imaging satellite launched by the German Aerospace Centre in June 2007. The onboard radar operating in the microwave X-band is capable of capturing images with high resolution, approx. 1 to 3 m, in the Spotlight and Stripmap modes, respectively, with changeable polarization. As described above, the acquisitions are independent of daylight and weather and can be obtained on demand. Table 1 summarizes the main features of TerraSAR-X.

Table 1 The main features of the TerraSAR-X satellite.

Radar frequency	9.65 GHz
Resolution	Spotlight – up to 1 m StripMap – up to 3 m ScanSAR – up to 18 m
Polarization	Single – HH, HV, VH, VV Dual – HH/HV, VV/VV, HH/VV
Incidence angle	20-55º
Scene size	Spotlight: 10 × 5 km StripMap: 30 × 50 km ScanSAR: 100 × 150 km
Revisit time	11 days
Launch date	15 June 2007 4:14 CEST
Orbital altitude	514 km

STUDY AREA

The research focuses on the agricultural lands of the Trzebnickie Hills which are classified as having moderate to very strong susceptibility to soil erosion by water (Fig. 2). Loess soils formed during the processes of denudation and aeolian accumulation in the Pleistocene period are dominant. The thickness of the loess layer ranges from 3.5 to 25 m (Szewrański & Żmuda, 2008). The relief is very diverse with slopes up to 25%. Soil erosion is observed during heavy spring and autumn rainfall, when the ground is sparsely covered with vegetation. Typical erosion features observed during field surveys include areas of sheet erosion dissected with rills and deep gullies.

In order to detect and identify the possible association between decreased coherence and soil erosion by water, anthropogenic sources of decorrelation must be eliminated. Any land treatment like tillage or harrowing leads to significant changes in radar backscattering. For this reason, a test site free of anthropogenic impact throughout the entire acquisition period was identified. The specific field is located around 16 km to the north of the centre of the city of Wroclaw (approximate coordinates of the central point of the field are: 51º15′00″N 17º06′40″E).

COHERENCE IMAGE GENERATION

Following (Lee & Liu, 2001) the coherence of two single look complex (SLC) radar images represents the local correlation of the radar reflection characteristics of the surface target between two observations, and is defined as:

$$\rho = \frac{|\langle I_1 I_2^* \rangle|}{[\langle I_1 I_1^* \rangle \langle I_2 I_2^* \rangle]^{1/2}}$$

where I_1, I_2 represent complex pixel values of the two images, $\langle\ \rangle$ denotes average over the neighbourhood, and * marks the conjugate of a complex number.

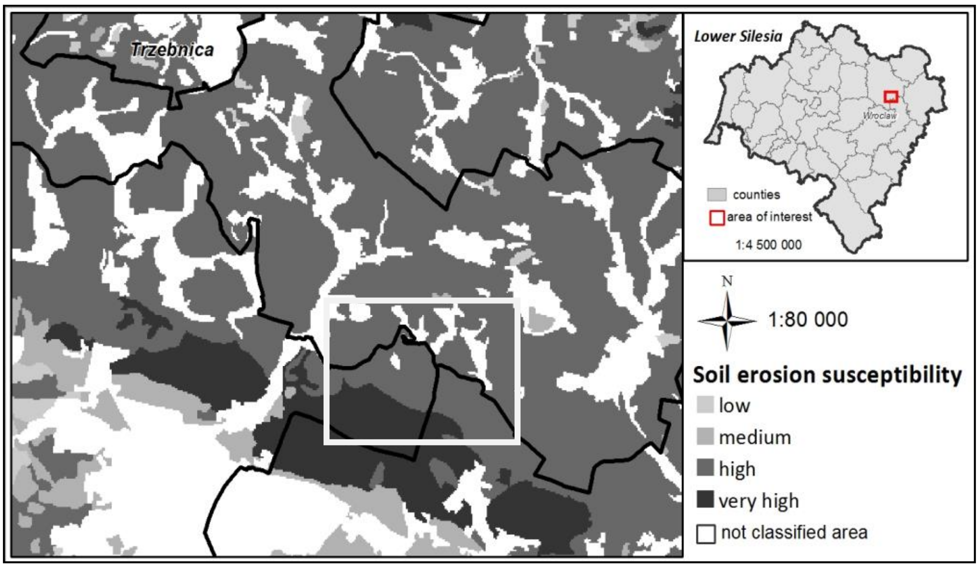

Fig. 2 Erosion susceptibility across the study area, showing the location of the test field. (Map source: Stuczyński, 2007).

As the time between image acquisitions grows, the temporal decorrelation becomes increasingly apparent, i.e. the correlation declines due to random changes of natural origin that happen on the surface. Apart from the temporal decorrelation, there are several other sources of coherence loss, including, amongst others:

(a) baseline or geometric decorrelation caused by the different incidence angles between image acquisitions;
(b) volume decorrelation due to the penetration of the radar waves in the scattering medium;
(c) system noise (e.g. Hanssen, 2001).

According to Lee and Liu (2001) the spatial component of decorrelation can be described as a function of the baseline and local terrain slope angle for a given radar look angle:

$$\rho = 1 - AB_{\perp}|ctg(\theta_0 - \alpha)|$$

where $A = c/\lambda r B_w$ is a constant for a SAR system; λ is the radar wavelength, r the slant range, c the speed of light and B_w the frequency bandwidth of the transmitted chirp signal; $B_{\perp}$ is the perpendicular component of baseline, θ_0 the nominal incidence angle of the radar and α the local terrain slope angle.

For a given baseline, the correlation decreases as the local slope angle approaches the nominal incidence angle. Consequently, for a given incidence angle, there exists a critical terrain slope above which the spatial correlation function reaches meaningless values (i.e. below zero). This fact must be taken into consideration when analysing coherence maps. In hilly areas, such as the study region, terrain slopes may reach the critical values and, consequently, generate lack of correlation. In soil erosion models, however, erosion hazard is also directly related to the local terrain slopes – generally the steeper the slope, the greater the risk of erosion (Table 2) Therefore, if decorrelation is to be used as a possible erosion indicator, it is essential to ensure that it is not primarily related to the critical terrain slope and the acquisition parameters must be chosen appropriately.

Parameters of the data used in this study (Table 3) guarantee that even the maximum slope recorded for the study area did not reach the critical values and, on this basis, spatial decorrelation caused by relief was not a problem for the data interpretation.

Table 2 Rates of the soil susceptibility to water soil erosion values on the basis of slope (Józefaciuk, 1999).

Soil type	<5%	6–10%	10–18%	18–27%	>27%
Loess soils	1	2	3	4	5

Table 3 TerraSAR-X acquisition parameters.

Acquisition date	Pass	Orbit	Polarization	Incidence angle
2-04-2011	DESC	21059	HH	~37º
5-04-2011	ASC	4382	HH	~37º
13-04-2011	DESC	21226	HH	~37º
16-04-2011	ASC	4549	HH	~37º
24-04-2011	DESC	21393	HH	~37º
27-04-2011	ASC	4716	HH	~37º

RESULTS AND ANALYSIS

Six images acquired between the 2nd and 27th April 2011 in StripMap mode (resolution of 3 m) were analysed to assess the potential for identifying soil erosion features from coherence maps. All the images had HH polarization due to its lower susceptibility to backscatter from vegetation, and an incidence angle of 37º to decrease image sensitivity to soil roughness (Baghdadi *et al*., 2002). Images were processed with the Delft Object-oriented Radar Interferometric software (DORIS) from the Delft University of Technology (Kampes *et al*., 2003). A total of four coherence maps were obtained from the following image pairings: 2.04-13.04 (Coh2-13), 13.04-24.04 (Coh13-24), 5.04-16.04 (Coh5-16) and 16.04-27.04 (Coh16-27).

Values assigned for coherence range from 0 (total lack of correlation) to 1 (full correlation). In the example coherence maps presented below, dark pixels represent areas of low coherence whereas brighter ones represent higher coherence. To detect presumptive regularities, the coherence maps were analysed visually and statistically in terms of the following attributes: terrain slope, precipitation and elevation.

A Digital Elevation Model (DEM) was used to obtain the elevation and calculate the slopes of the study area. The DEM was derived from aerial photography (1:26 000) and had a resolution of 10 m which was interpolated to match the 3 m resolution of the SAR images. The key features of the terrain for the study area are shown in the elevation contour map in Fig. 3.

Precipitation data for April 2011 was collected from a raingauge situated approx. 10 km north from the study area. Figure 4 shows the timeline of the image acquisitions overlain with the distribution of precipitation. A significant decrease in coherence, especially in the northern, middle and southeastern parts of the study area is observed in all four maps. Since the study field was selected on the basis of the lack of human activity (e.g. tillage) and sparse vegetation cover, the decorrelation can only be attributed to natural factors such as precipitation and soil denudation. However, the weather conditions did not appear to play a substantial role in generating the evolution of the correlation since there was no obvious link between rainfall and the decorrelation, with the possible exception of the last image which was taken shortly after a heavy storm event.

Coherence was compared with the topographical features obtained from the DEM. The terrain slopes were divided into five classes with corresponding soil erosion ratings (cf. Józefaciuk, 1999). Accordingly, the coherences were classified as very low (coherence value 0–0.2), low (0.2–0.4), medium (0.4–0.6), high (0.6–0.8) and very high (0.8–1.0). Areas with steep slopes and low coherence were identified using the visual interpretation of classified images (Fig. 5).

Detailed comparison with the DEM suggested that areas of lower coherence are either steep slopes (e.g. the northern and central part of the study area) or terrain depressions (e.g. the central and southeastern part of the study area). Field observations (see photographs in Fig. 6) confirmed that the depressions are areas where sediments from the upslope portions of the field are accumulating. Further analysis examined the relationship between coherence and relief and the results for the coherence maps are presented in Table 4. In these cases the correlation coefficient ranged between –0.32 to –0.54, thereby suggesting a statistically robust level of correlation.

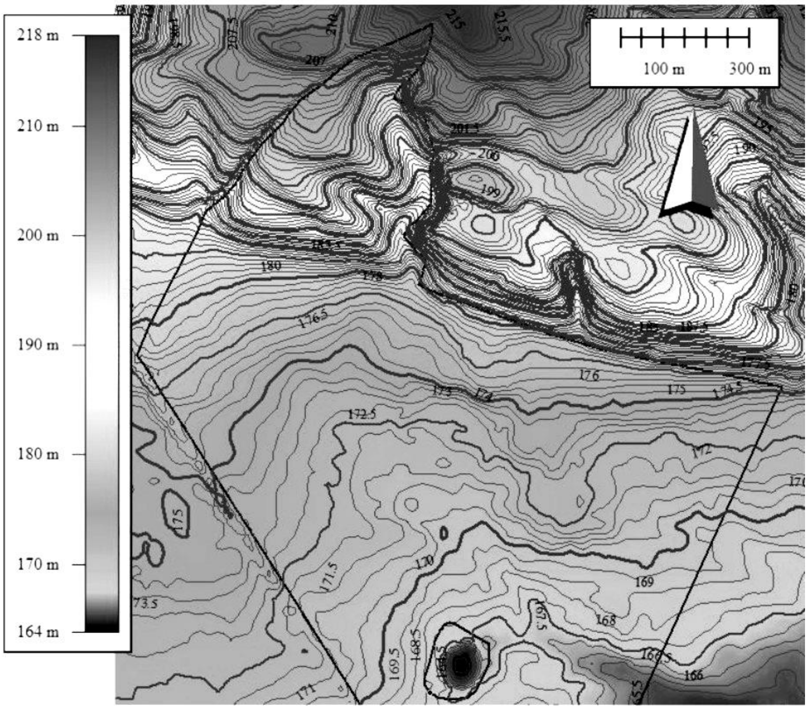

Fig. 3 Digital Elevation Model of the study area with height contours.

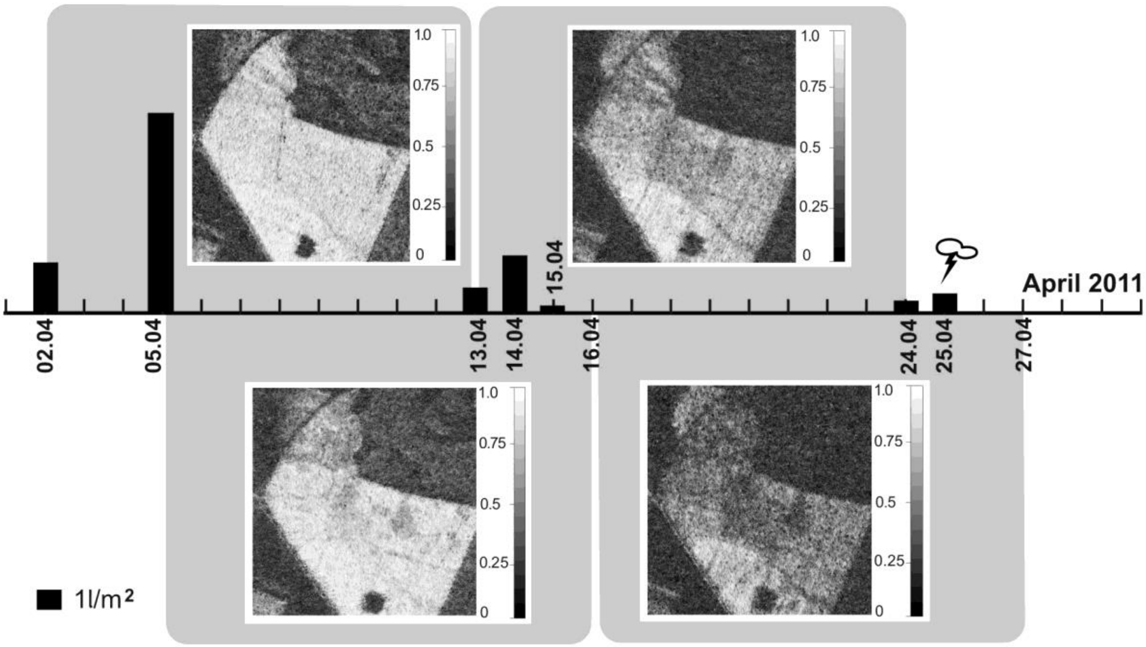

Fig. 4 Coherence maps starting from top left: Coh2-13, Coh13-24, Coh5-16 and Coh16-27 and the corresponding precipitation during April 2011.

Table 4 Correlation coefficients between coherence and slope.

Coherence map	Correlation with slope
Coh2-13	–0.41
Coh13-24	–0.34
Coh5-16	–0.54
Coh16-27	–0.32

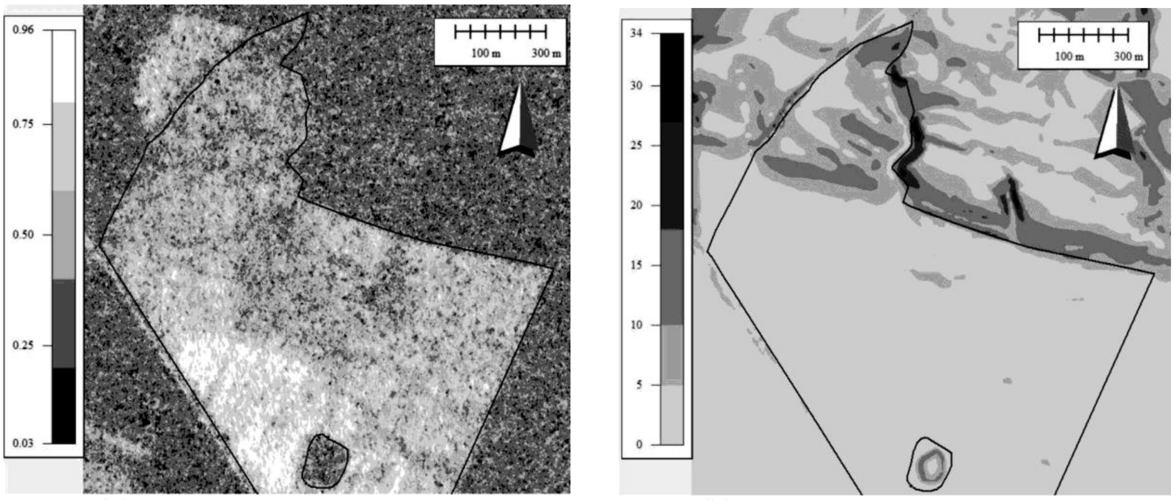

(a) (b)

Fig. 5 (a) Classification of the coherence image, Coh16-27; and (b) classification of slopes.

Fig. 6 Eroded soil in the study field.

In addition to the correlation analysis, linear regression was performed between the slope and decorrelation. In all four cases the coherence was clearly inversely proportional to the slope steepness and the coefficient of proportionality for the normalized slope (i.e. expressed as a fractional value between 0 and 1) varied between –1.5 and –2.5. An example graph for one of the correlation maps (Coh2-13) is shown in the Fig. 7.

CONCLUSIONS

Obtaining reliable data on the spatial extent of soil erosion by water, especially at larger spatial scales, is very expensive and time-consuming. Supporting existing assessment methods with the use of satellite imaging appears to be very promising, especially in terms of reducing the costs of data acquisition. There are, however, certain limitations to take into account. First and foremost is the underlying assumption that there is no significant anthropogenic impact on the target area. Additionally, it is desirable that the vegetation is sparse throughout the whole period of data

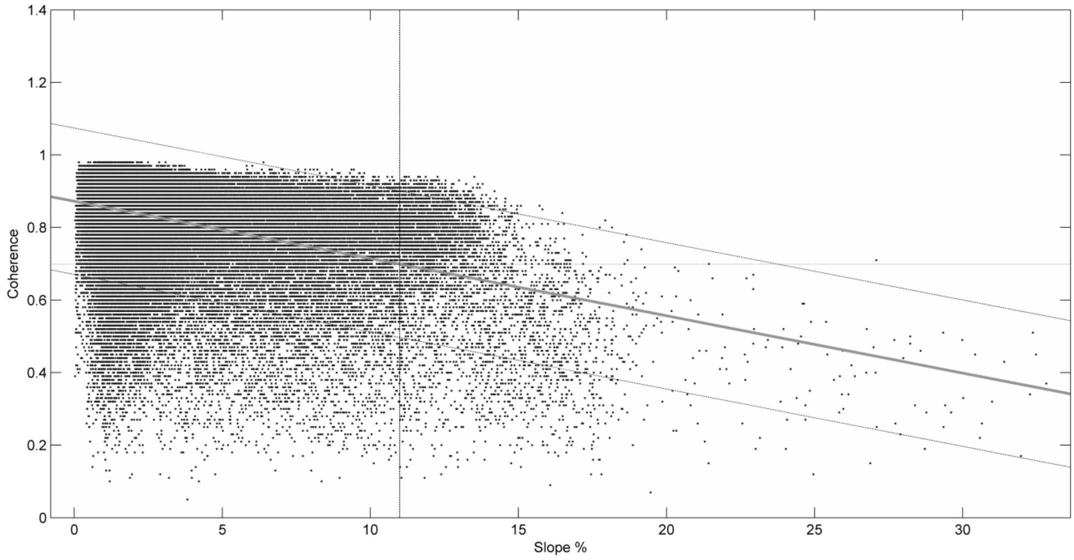

Fig. 7 Correlation between slope and coherence for Coh2-1.

acquisition. If these key conditions are met, the measured change in coherence can only be attributed to natural sources and may indeed indicate soil erosion processes. However, this limits the practical application of the method to one, maximum two, months in a year (March–April in the Northern Hemisphere) when the land is exposed to direct radar measurements and significant crop growth has not started yet – or to areas totally unused by agriculture. The use of satellite imagery needs to be supplemented with supportive data, e.g. from soil maps and on moisture content. Future work will compare the results obtained in this study with the newly acquired TerraSAR-X coherence maps, completed with ground truth data and existing soil and erosion hazard maps.

Acknowledgements The research presented in this paper was funded by the Polish Ministry of Science and Higher Education (from Funds on Science in 2009–2012 as a research project number N N526 246138). The work was supported by the Wroclaw Centre of Networking and Supercomputing using Matlab Software License no: 101979. The TerraSAR-X data used in this study were obtained under the user license LAN0514.

REFERENCES

Baghdadi, N., King, C., Bourguignon, A. & Remond, A. (2002) Potential of ERS and Radarsat data for surface roughness monitoring over bare agricultural fields: application to catchments in Northern France. *Int. J. Remote Sens.* 23(17), 191–198.

Hanssen, R. F. (2001) *Radar Interferometry: Data Interpretation and Error Analysis.* Kluwer Academic Publishers, Boston.

Józefaciuk, A.& Józefaciuk, Cz. (1999) *Ochrona gruntów przed erozją.* Wydawnictwo IUNG, Puławy, Poland.

Kampes, B., Hanssen, R. & Perski, Z. (2003) Radar interferometry with public domain tools. *Proc. FRINGE 2003*, Frascati, Italy.

Lee, H. & Liu, J. G (2001) Analysis of topographic decorrelation in SAR interferometry using ratio coherence imagery. I*EEE Trans. Geoscience and Remote Sensing* 39(2), 223–232.

Massonnet, D. & Feigl, K. L. (1998) Radar interferometry and its application to changes in the Earth's surface. *Rev. Geophys.* 36(4), 441–500.

Perski, Z. (2000) The interpretation of ERS-1 and ERS-2 INSAR data for the mining subsidence monitoring in Upper Silesian coal basin, Poland. *International Archives of Photogrammetry and Remote Sensing* XXXIII, Part B7, 1137–1141.

Rabus, B., Eineder, M., Roth, A. & Bamler, R. (2003) The shuttle radar topography mission – a new class of digital elevation models acquired by spaceborne radar. *Photogramm. Rem. Sens.*57, 241–262.

Stuczyński, T. *et al.* (2007) Stan i zmiany właściwości gleb użytkowanych rolniczo w województwie dolnośląskim w latach 2000–2005. *Urząd Marszałkowski woj. Dolnośląskiego –- IUNG Puławy*, Wrocław-Puławy, Poland

Szewrański, Sz. & Żmuda, R. (2008) *Prognozowanie efektów spowodowanych wprowadzeniem zasad dobrych praktyk rolniczych.* Wydawnictwo Uniwersytetu Przyrodniczego we Wrocławiu, Poland.

Vrieling, A. (2006) Satellite remote sensing for water erosion assessment: A review. *Catena* 65, 2–18.

Wegmuller, U., Strozzi, T., Farr, T. & Werner, C. L. (2000) Arid land surface characterization with repeat-pass SAR interferometry. *IEEE Trans. Geoscience and Remote Sensing* 38, 776–781.